

Electronegativity Seen as the Ground-State Average Valence Electron Binding Energy

Martin Rahm,^{*,†} Tao Zeng,[‡] and Roald Hoffmann[§]

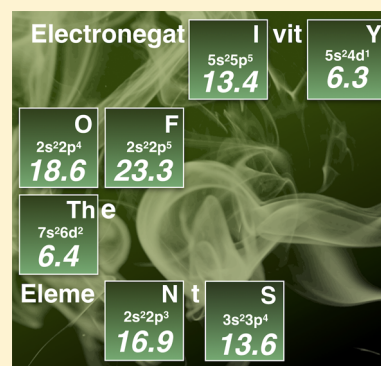
[†]Department of Chemistry and Chemical Engineering, Chalmers University of Technology, SE-412 96, Gothenburg, Sweden

[‡]Department of Chemistry, Carleton University, Ottawa, Ontario K1S 5B6, Canada

[§]Department of Chemistry and Chemical Biology, Cornell University, Ithaca, New York 14853, United States

Supporting Information

ABSTRACT: We introduce a new electronegativity scale for atoms, based consistently on ground-state energies of valence electrons. The scale is closely related to (yet different from) L. C. Allen's, which is based on configuration energies. Using a combination of literature experimental values for ground-state energies and *ab initio*-calculated energies where experimental data are missing, we are able to provide electronegativities for elements 1–96. The values are slightly smaller than Allen's original scale, but correlate well with Allen's and others. Outliers in agreement with other scales are oxygen and fluorine, now somewhat less electronegative, but in better agreement with their chemistry with the noble gas elements. Group 11 and 12 electronegativities emerge as high, although Au less so than in other scales. Our scale also gives relatively high electronegativities for Mn, Co, Ni, Zn, Tc, Cd, Hg (affected by choice of valence state), and Gd. The new electronegativities provide hints for new alloy/compound design, and a framework is in place to analyze those energy changes in reactions in which electronegativity changes may not be controlling.



INTRODUCTION

Electronegativity is one of the most important chemical descriptors, important, not only because it assigns a measure to the propensity of atoms in molecules to attract electrons but because it has been productively employed, on countless occasions, to guide molecular and material design. The concept itself has many definitions^{1–17} and a rich history reaching back to Berzelius.^{18–20} Most electronegativity scales, including ours here, cover only parts of the periodic table, typically omitting various heavy or heaviest elements.

We present here a new scale of electronegativity that covers all atoms from hydrogen to curium, 1–96. The approach follows previous work by two of us (M.R. and R.H.),^{21,22} in turn based on ideas of L. C. Allen, where we addressed electronegativity in the context of the average electron energy, $\bar{\chi}$. One advantage of the quantity $\bar{\chi}$ is that changes in it can be related to the total energy change of a system by the equation

$$\Delta E = n\Delta\bar{\chi} + \Delta V_{\text{NN}} - \Delta E_{\text{ee}} \quad (1)$$

where n is the total number of electrons, V_{NN} is the nuclear–nuclear repulsion energy (=zero for an atom), and E_{ee} quantifies the average multielectron interactions (in previous work we referred to $-E_{\text{ee}}$ as ω), which is complementary to the mean-field interelectron interaction in the Fock operator.^{21,22} Because total energy changes determine the outcome of many chemical or physical processes, it is helpful to decompose that energy in familiar terms, such as electronegativity. For example, when the terms of eq 1 are considered in the course of a chemical bond formation, ΔE equals the bond energy, and $\Delta\bar{\chi}$

can be interpreted as either the corresponding average orbital or electron stabilization, or electronegativity equalization.^{21,22}

As was shown in previous work, the $\Delta\bar{\chi}$ part of the energy change need not be negative for an exothermic reaction. When it is not, the transformation is instead driven by changing multielectron effects, which is indicative of polar, ionic, and metallogenic bonding.^{21,22}

ELECTRONEGATIVITY AS THE AVERAGE BINDING ENERGY OF VALENCE ELECTRONS

$\bar{\chi}$ can, in principle, be experimentally estimated for any system, and it can be quantum mechanically calculated using a variety of methodologies.^{21,22} For example, $\bar{\chi}$ can be estimated as the average of the energies of all occupied orbitals or as an average of ionization energies, which can be either calculated or experimentally measured,

$$\bar{\chi} = \frac{\sum_{i=1}^n n_i \varepsilon_i}{n} \quad (2)$$

where ε_i is the energy of the i th level, n_i is the occupation the i th level, and n is the total number of electrons. Please note that in order for $\bar{\chi}$ values to be applicable together with eq 1, which describes the total energy, the energy reference for ε_i in eq 2 needs to be vacuum. $\bar{\chi}$ is, in other words, negative for bound systems under ambient conditions. However, we will in this work present $\bar{\chi}$ as positive numbers. This sign change is done

Received: September 21, 2018

Published: November 30, 2018

to facilitate discussion and comparison with experimental ionization potentials of atoms, which are positive by definition.

Whereas previous work by some of us focused on $\Delta\bar{\chi}$ and its use in analyzing chemical bonding, it is important to note that numerical values of $\bar{\chi}$ can only be directly compared to traditional scales of electronegativity when the average energy, eq 2, is calculated by summing only over the valence electrons. Otherwise the $\bar{\chi}$ values are increasingly larger, dominated by the core energies. When one restricts the sum to the valence orbitals, we arrive at an approximation (it will soon become clear how our scale differs) to Allen's electronegativity scale.^{10,23–25} This scale agrees (it correlates linearly and quite well) with most other scales of electronegativity.²⁶ For this reason, we will in the rest of this work refer to $\bar{\chi}$ as a valence-only average, unless otherwise specified. In doing so, we keep in mind that $\bar{\chi}$'s relation to the total energy, eq 1, only holds for all-electron averages $\bar{\chi}$ (we will examine this point in detail in future work). Equation 1 still holds approximately for valence-only averages and is useful for qualitative predictions, provided that core level shifts are not too important and the true $\Delta\bar{\chi}$ can be reasonably well estimated from the change of valence levels.

One immediately encounters a conceptual difficulty. What is considered a “valence” level and what is a “core” one is to a certain extent a matter of definition and preference. We know that the energy of the outermost levels varies with charge on the atom and that these energy spacings between levels decrease with increasing atomic number down the periodic table. Here we define “valence” in five different ways in various parts of the periodic table, four of them generally uncontroversial.

1. For the alkali metal and alkaline earth atoms, the s-block, we use the highest occupied s-level of atoms.
2. For what are usually labeled main-group elements, the p-block atoms, only the outermost s- and p-levels are considered.
3. For the d-block, labeled colloquially the transition metals, $\bar{\chi}$ is calculated from the outermost s- and d-levels.
4. For atoms in the f-block (lanthanides and actinides), the highest lying s-, d-, and f-levels are all included when calculating $\bar{\chi}$.
5. The problem, and not just for us, is group 12. It is obvious that these elements should present a problem, for they are truly “in-between”. In them and their compounds the nd block is clearly below $(n + 1)$ s and p. In contrast, small s–d gaps and the existence of +III or higher oxidation states have been confirmed for all other d-block atoms, groups 3–11. For example, atoms of group 11, Cu, Ag, and Au, show s–d binding energy differences of 2.7, 4.9, and 1.9 eV, respectively. In groups 3–11, nd orbitals are clearly part of the valence set. Just as clearly they are not part of the valence set in groups 13–18 (our considerations exclude the wonderful realm of matter under high pressure, where things can be different, to put it mildly). Group 12 elements will have the nd levels flirting with being part of the valence set, causing problems for the poor theoreticians trying to cram them into one or the other category. Zinc and cadmium exhibit relatively large d–s gaps of 7.8 and 8.6 eV, and these two elements are usually considered part of a post-transition-metal group.²⁷ Their highest

experimentally determined oxidation states are +II,²⁸ and computational predictions ensure us that higher oxidation states are unlikely to be found.²⁹ In contrast, mercury, the last element of group 12, has a smaller s–d gap of 4.4 eV and can exhibit an oxidation state of up to +4, in HgF₄.³⁰

Here is our resolution: We treat all atoms of group 12 on equal footing with all other d-block atoms and define their electronegativity by an s^2d^{10} valence configuration. This results in these elements taking the highest electronegativities of the d-block. High electronegativities of group 12 do have merits and will be discussed. For those uneasy with our preferred definition, we also provide electronegativity values based on an s^2 valence set for group 12 atoms, where we consider the d^{10} subshell as part of the core (and therefore not added into the definition of the electronegativity).

For practical reasons that will be discussed, we include one further criterion in our definition of electronegativity: only the ground electronic states occupied at $T \rightarrow 0$ K are considered. Why this is necessary will become clear after comparing our scale with that of Allen.

■ USING THE GROUND STATE AS A REFERENCE

Allen's electronegativity scale^{10,23–25} has been a major inspiration for our work, yet his definition differs from ours in some principal aspects. First, Allen's scale does not consider atomic ground states (those that are occupied at $T \rightarrow 0$ K). Rather it relies on configurational averages. In other words, for each electronic configuration required to calculate the average ionization energy, an average is taken over all L – S terms and all the J levels derived from the L – S terms. A comparison between ours and Allen's approach is exemplified in Figure 1, in which energies of the sublevels of the $2s^22p^2$ configuration of the C atom and the $2s^22p^1$ and $2s^12p^2$ configurations of the C⁺ cation produced in the ionizations are shown.

Allen's approach is unproblematic for light elements such as carbon, since the number of $^{2S+1}L_J$ levels is relatively small and all of them have been identified in their atomic spectra. However, atomic spectra and configurational average computations become more and more complex as the atoms become heavier. The number of microscopic states, and thus the numbers of L – S terms and J levels, can be very large for the f-block elements. An extreme example is the $4f^75d^16s^1$ ground state configuration of the Gd cation, which gives rise to 45 760 microscopic states. It is difficult, if not impossible, to identify all these levels in a spectrum and average them. It is also difficult to handle such a large number of states in calculations. An example of how we calculate $\bar{\chi}$ for Gd is shown in the Supporting Information.

This is likely the reason that the Allen scale was never extended to include the f-block elements. It is also the reason that we here forego Allen's configurational average approach in favor of a more straightforward ground-state-based definition of electronegativity. We note that we are not the first to encounter the difficulty in finding all relevant J levels in the atomic spectra. For instance, Roos et al. pointed out that “It is difficult to compare to J -averaged data in many cases due to lacking experimental information in particular for the positive ions”, in their calculations of f-block atoms' first ionization potentials.³¹ Considering that Roos et al. only needed all J levels for one L – S term of one atomic and one cationic configuration, while Allen's scheme requires all J levels for all

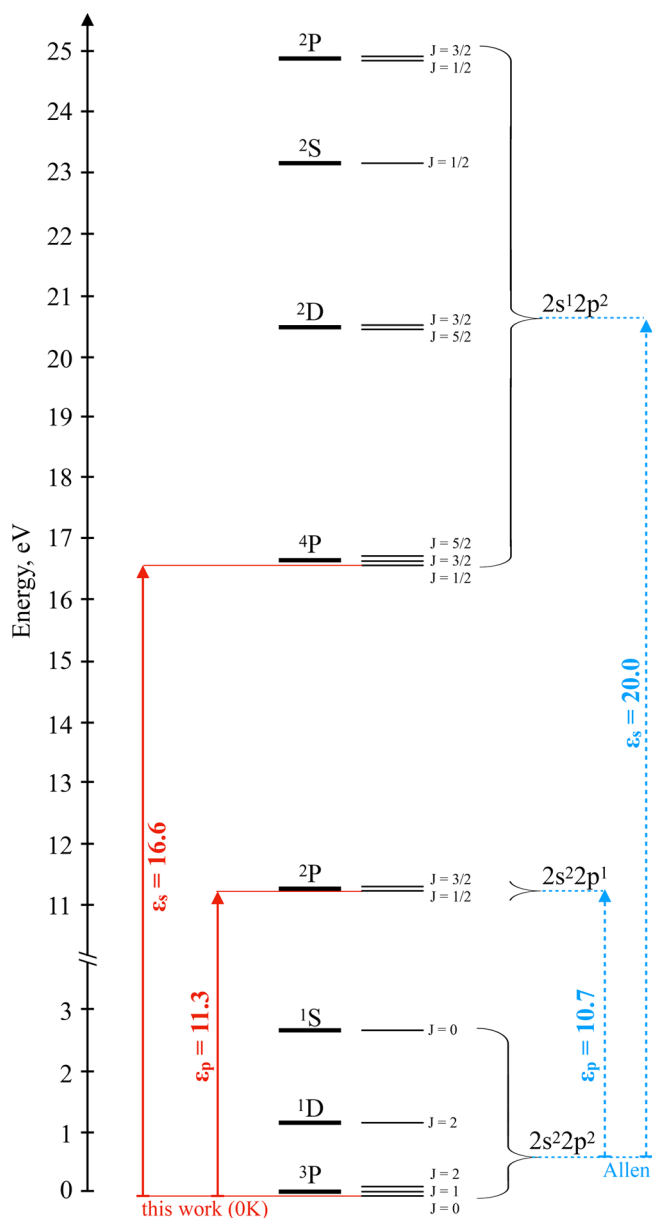


Figure 1. Energies of the L - S terms and J levels of atomic and cationic carbon obtained from NIST sources. J -levels are not drawn to proper energy scale. In this work, electronegativity is calculated as an average of valence electron binding energies of atoms in their ground state ($T \rightarrow 0$ K) according to eq 2. For carbon, this requires estimates of the $2s$ and $2p$ ionization energies, ϵ_s and ϵ_p , which are shown in red. This approach of estimating the valence ionization energies is different from the Allen scale of electronegativity, shown in blue, in which full averages over all J levels of the atomic and cationic configurations are performed, respectively. The location of the peak of the curly bracket enclosing the $2s^2 2p^2$ levels reflects the larger weight of the 3P term in this average. The resulting electronegativity of carbon emerges as 15.3 and 13.9 eV e^{-1} using the Allen definition and our ground-state definition, respectively.

L - S terms of one atomic and several cationic configurations, it is simply unworkable to extend Allen's scheme to the f-block elements.

In arriving at our data, we have followed a hybrid approach and relied whenever possible on experimental measurements of valence electron binding energies available through the NIST Atomic Spectra Database. For atoms where sufficiently

accurate data are missing, corresponding ionization energies have instead been calculated, as described in the Methodology section.

■ COMPARISON TO THE ALLEN ELECTRONEGATIVITY SCALE

The Allen scale covers 72 atoms of the periodic table, which allows for a rather comprehensive comparison with other electronegativity definitions. As we shall see, adopting our ground-state definition has a relatively small effect on relative trends in electronegativity, when compared to the LS and J -averaging of Allen. Like the example of carbon shown in Figure 1, our ground-state scale mostly portrays elements as being more electropositive than in the Allen scale. Of course, since the offset occurs for most elements, this means that relative orderings are largely unchanged. The few exceptions to this rule, where deviations are instead positive, are all found in the d-block and will be discussed separately. Figure 2 shows the linear correlation between the ground-state scale presented in this work and the Allen electronegativities.

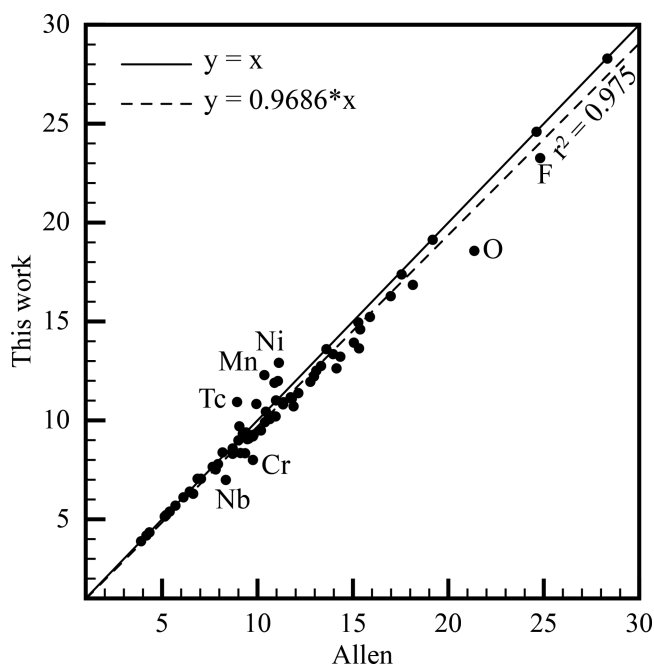


Figure 2. Comparison between the ground-state ($T \rightarrow 0$ K) electronegativity scale of this work with that of Allen, for the 69 atoms where a comparison is possible (Zn, Cd, and Hg are omitted; see text for discussion). The axes show valence electron binding energies in eV e^{-1} . One Pauling unit $\approx 6 \text{ eV e}^{-1}$.^{25,33} The standard deviation for the full data set is 0.88 eV e^{-1} (or 9.3%).

Overall, and as expected from the above argument, our estimated electronegativities are smaller than those of Allen's, as reflected by the 0.9686 slope in the linear fitting of our values against Allen's (Figure 2). The reason for our smaller values is clearly illustrated in Figure 1, which demonstrates a larger splitting between L - S terms in the $2s^1 2p^2$ cationic configuration than in the $2s^2 2p^2$ atomic configuration. Cations tend to have such larger splittings. This is because the splitting is induced by Coulombic interactions between valence electrons,³² and in cations, the valence orbitals are more contracted, resulting in stronger multielectron interactions. The larger splittings will generally raise the center of gravity of

Electronegativity of the Atoms																										
Average valence electron binding energy as $T \rightarrow 0\text{K}$ eV e^{-1}																										
1	2													13	14	15	16	17	18							
1	H 1s ¹ 13.6																			He 1s ² 24.6						
2	Li 2s ¹ 5.4	Be 2s ² 9.3													B 2s ² 2p ¹ 11.4	C 2s ² 2p ² 13.9	N 2s ² 2p ³ 16.9	O 2s ² 2p ⁴ 18.6	F 2s ² 2p ⁵ 23.3	Ne 2s ² 2p ⁶ 28.3						
3	Na 3s ¹ 5.1	Mg 3s ² 7.6													Al 3s ² 3p ¹ 9.1	Si 3s ² 3p ² 10.8	P 3s ² 3p ³ 12.8	S 3s ² 3p ⁴ 13.6	Cl 3s ² 3p ⁵ 16.3	Ar 3s ² 3p ⁶ 19.1						
4	K 4s ¹ 4.3	Ca 4s ² 6.1	Sc 4s ² 3d ¹ 7.0	Ti 4s ² 3d ² 8.4	V 4s ² 3d ³ 9.7	Cr 4s ¹ 3d ⁵ 8.0	Mn 4s ² 3d ⁵ 12.3	Fe 4s ² 3d ⁶ 10.1	Co 4s ¹ 3d ⁷ 11.9	Ni 4s ² 3d ⁸ 12.9	Cu 4s ¹ 3d ¹⁰ 10.2	Zn 4s ² 3d ¹⁰ 15.9	Ga 4s ² 4p ¹ 9.9	Ge 4s ² 4p ² 11.1	As 4s ² 4p ³ 12.5	Se 4s ² 4p ⁴ 13.2	Br 4s ² 4p ⁵ 15.2	Kr 4s ² 4p ⁶ 17.4								
5	Rb 5s ¹ 4.2	Sr 5s ² 5.7	Y 5s ² 4d ¹ 6.3	Zr 5s ² 4d ² 7.5	Nb 5s ¹ 4d ⁴ 7.0	Mo 5s ¹ 4d ⁵ 8.3	Tc 5s ² 4d ⁵ 10.9	Ru 5s ¹ 4d ⁷ 8.4	Rh 5s ¹ 4d ⁸ 9.3	Pd 4d ¹⁰ 8.3	Ag 5s ¹ 4d ¹⁰ 12.0	Cd 5s ² 4d ¹⁰ 16.1	In 5s ² 5p ¹ 9.3	Sn 5s ² 5p ² 10.2	Sb 5s ² 5p ³ 11.2	Te 5s ² 5p ⁴ 12.0	I 5s ² 5p ⁵ 13.4	Xe 5s ² 5p ⁶ 14.9								
6	Cs 6s ¹ 3.9	Ba 6s ² 5.2	Lu 6s ² 5d ¹ 6.4	Hf 6s ² 5d ² 7.1	Ta 6s ² 5d ³ 7.8	W 6s ² 5d ⁴ 8.6	Re 6s ² 5d ⁵ 9.1	Os 6s ² 5d ⁶ 9.2	Ir 6s ² 5d ⁷ 10.8	Pt 6s ¹ 5d ⁹ 9.5	Au 6s ¹ 5d ¹⁰ 10.9	Hg 6s ² 5d ¹⁰ 14.1	Tl 6s ² 6p ¹ 10.2	Pb 6s ² 6p ² 11.0	Bi 6s ² 6p ³ 10.7	Po 6s ² 6p ⁴ 12.2	At 6s ² 6p ⁵ 12.6	Rn 6s ² 6p ⁶ 14.6								
7	Fr 7s ¹ 4.1	Ra 7s ² 5.3																								
6	La 6s ² 5d ¹ 6.0	Ce 6s ² 4f ¹ 5d ¹ 7.3	Pr 6s ² 4f ³ 6.7	Nd 6s ² 4f ⁴ 7.2	Pm 6s ² 4f ⁵ 7.4	Sm 6s ² 4f ⁶ 8.3	Eu 6s ² 4f ⁷ 9.4	Gd 6s ² 4f ⁷ 5d ¹ 13.8	Tb 6s ² 4f ⁹ 7.7	Dy 6s ² 4f ¹⁰ 8.4	Ho 6s ² 4f ¹¹ 8.3	Er 6s ² 4f ¹² 7.6	Tm 6s ² 4f ¹³ 9.0	Yb 6s ² 4f ¹⁴ 10.2	Element ground state valence configuration $\bar{\chi}$											
7	Ac 7s ² 6d ¹ 5.8	Th 7s ² 6d ² 6.4	Pa 7s ² 5f ² 6d ¹ 6.3	U 7s ² 5f ³ 6d ¹ 7.5	Np 7s ² 5f ⁴ 6d ¹ 8.2	Pu 7s ² 5f ⁶ 7.3	Am 7s ² 5f ⁷ 8.3	Cm 7s ² 5f ⁷ 6d ¹ 10.9																		

Figure 3. Electronegativity of atoms 1–96. All data are compiled from the NIST Atomic Spectra Database, except for atoms Tc, Os, Po–Rn, La–Yb, and Pa–Cm, for which the electronegativity estimate to varying degrees relies on quantum mechanical calculations described in the [Methodology](#) section. Note that including the d^{10} shell in the valence of Zn, Cd, and Hg is debatable. If only the s^2 configuration of Zn, Cd, and Hg were to be considered part of the valence, their electronegativities would instead be 9.4, 9.0, and 10.4 eV e^{-1} , respectively. One Pauling unit $\approx 6 \text{ eV e}^{-1}$.^{25,33}

the cationic $L-S$ terms from the cationic lowest $L-S$ term, more than the center of gravity of the atomic $L-S$ terms is raised above the atomic lowest $L-S$ term. Our ground-state scheme hence leads to generally lower (in absolute terms) electronegativities than Allen's.

■ VALENCE-ONLY ELECTRONEGATIVITIES

Our revised and extended set of electronegativities for atoms 1–96 is summarized in [Figure 3](#). We are limited to 96 elements because the type of basis set that we employed is not available for the still heavier elements.

Most of the data in [Figure 3](#) will come as no surprise to chemists, as the general trends are the same as in most other scales in the literature. The units are naturally those of energy, as they are for Allen and Mulliken electronegativities. If the reader wishes to have a rough conversion to the time-honored Pauling scale, 1 Pauling unit $\approx 6 \text{ eV e}^{-1}$.^{25,33} A comparison with the Mulliken scale, as revised by Cárdenas, Heidar-Zadeh, and Ayers,³⁴ can be found in the [Supporting Information](#). The paper cited actually estimates the chemical potential, whose negative can be identified with Mulliken electronegativity. Our scale and the Mulliken one are in qualitative agreement. However, there are significant differences between the two scales. Some occur where expected, as for group 12. The coefficient of determination (r^2) of a linear regression between our and the Mulliken scale is 0.82 ([Figure S1](#)).

There are some examples in this revision and expansion of electronegativity that merit special comment. We will first focus our discussion on the largest outliers compared to the Allen scale ([Figure 2](#)) and then address the new data presented for the f-block and some other heavy elements. We begin in the

main group—and two important atoms for chemistry—oxygen and fluorine.

■ OXYGEN

On comparing the energies of Allen's original scale to our ground-state scale, oxygen is by far the largest outlier. In Allen's configurational average definition of electronegativity, oxygen has a value of 21.4 eV e^{-1} . In contrast, as $T \rightarrow 0 \text{ K}$, the average energy computed from the $2s^2 2p^4$ (3P_2) $\rightarrow 2s^2 2p^3$ ($^4S_{3/2}$) and the $2s^2 2p^4$ (3P_2) $\rightarrow 2s^2 2p^4$ ($^4P_{5/2}$) ionizations that now describe the valence levels is equal to 18.6 eV e^{-1} . The difference is -2.8 eV e^{-1} , or approximately half of one Pauling unit. What consequences does this have?

One important use of electronegativity is that its difference between two atoms can be taken as a predictive indicator for their reactivity with one another. If one atom has a sufficiently higher electronegativity than another, it has the potential to withdraw electron density from its neighbor and to oxidize the other atom. However, the noble gas elements are special in this sense. They have a closed-shell electronic structure and a nonexistent electron affinity, which means that they typically do not oxidize other elements. For noble gas elements, their high electronegativity ([Figure 3](#)) indicates how well they resist oxidation. For this reason, we will single out examples of noble gas reactivity in the following discussion of outliers.

The new value for oxygen's electronegativity (18.6 eV e^{-1} , cf. [Figure 3](#)) makes it less electronegative than argon (19.1 eV e^{-1}) and just above krypton (17.4 eV e^{-1}). This value is in better accord with experimental observation, since it does not imply the possibility of argon oxides. Krypton oxides do not exist, although they have been predicted to be stable above approximately 300 GPa.³⁵ Such predictions are in accord with

a small electronegativity difference between oxygen and krypton at 1 atm and imply that the electronegativity of oxygen relative to krypton increases under compression. We will report on the explicit effect of pressure on electronegativity in a separate publication. Taken at face value, Allen's original value of 21.4 eV e^{-1} for the electronegativity of oxygen erroneously implies that the element should be able to oxidize both of these noble gases under ambient conditions.

Another noble gas comparison is with xenon. The electronegativity of xenon is 14.9 eV e^{-1} , and metastable xenon oxides can be synthesized; both our and Allen's scale agree here. Of course, almost every other element in the periodic table can be oxidized by oxygen, and we will not discuss any more such combinations other than to say that all elements, except helium, neon, argon, and fluorine, are less electronegative than oxygen.

■ FLUORINE

Fluorine is the most electronegative reactive element of the periodic table, a fact that has been utilized to create a plethora of strong oxidizers and superacids,³⁶ remarkable oxofluoride compounds such as ClF_3O_2 ,³⁷ unusual structures, such as pentagonal planar XeF_5^- ,³⁸ and a large variety of fluorinated carbon compounds.^{39–42} Fluorine is our second largest outlier in the main group (Figure 2), differing by -1.6 eV e^{-1} from its value on Allen's scale. As for oxygen, our scale thus portrays fluorine as slightly less electronegative, in an absolute sense. The most apparent relative difference is that fluorine now is 1.3 eV e^{-1} less electronegative than helium. This is in contrast to the Allen scale, which predicts fluorine to be *more* electronegative than helium by 0.2 eV e^{-1} . Our revised values, shown in Figure 3, can be thought of as being in better agreement with the existence of species such as krypton difluoride⁴³ and argon fluorohydride⁴⁴ and the nonexistence of helium fluorides (we are here omitting transient cationic species and weakly bound anionic species). The slightly lowered electronegativity of fluorine presented here may be of consequence when evaluating the stability, or instability, of some hitherto nonexistent exotic fluorides.

■ THE D-BLOCK

A direct comparison with the Allen electronegativity for the d-block is not possible. The reason is that Allen did not follow his original experimentally accessible definition¹⁰ when addressing the d-block elements.⁴⁵ The number of d-level electrons to be included in Allen's configurational average was not given by the ground-state electron configuration. Instead, the largest known formal oxidation state was used to count the number of d-electrons included in the valence.

This is problematic, since the maximal known formal oxidation state for several atoms has changed over time. For example, Allen lists the maximum oxidation state for iron as +6, which leads to 4 "active" d-electrons in the valence shell. However, the maximum oxidation state can be +7,⁴⁶ or even up to +8.^{47,48} Another example is iridium, also listed as having a maximum oxidation state of +6. That record has since been broken by the detection of both Ir(VIII) in IrO_4 ⁴⁹ and Ir(IX) in $[\text{IrO}_4]^+$.⁵⁰ We really do not want to enter the contentious discussion of oxidation states and what is or is not stable. It is clear that Allen's choices need to be revisited. In addition to adding the oxidation state constraint, Allen also employed a special kind of relativistic Hartree–Fock calculations to derive

partial orbital occupancies; that method was then used to further modify the number of considered d-level electrons.

In our approach, we maintain the same definition over the entire periodic table and calculate $\bar{\chi}$ over all highest occupied s- and d-levels of the same principal quantum number. Despite a significantly more straightforward approach, and no use of calculations except for the d-binding energy of Tc and Os, the agreement with Allen's scale is rather good. The standard deviation over all d-block elements (when we omit Zn, Cd, and Hg) is 0.88 eV e^{-1} (or 9.3%). Because of the inherently different definitions for the d-block, we will not linger on the differences. Nevertheless, it is interesting to point to some of the outliers in the context of their chemistry. Whereas we will not compare to the classical Pauling scale, except in certain instances, the interested reader is welcome to do so. We again remind one that one Pauling unit translates as approximately 6 eV e^{-1} .^{25,33}

These revised transition metal electronegativities do allow for a few predictions. Certain d-block atoms come out as more electronegative than some p-block elements and very near to others. For example, Ni, Co, and Mn all have higher electronegativities than the atoms in groups 13 and 14, with the exception of carbon, and higher than Sb and Bi in group 15. Could this allow for the existence of binary alloys where a p-block atom is oxidized and the d-block atom is reduced? Electron density measurements (and calculations) of the important thermoelectric material CoSb_3 have already indicated that Co can take on a negative charge in this alloy.⁵¹

■ COPPER, SILVER, AND GOLD

A noteworthy difference is in the relative ordering of electronegativities in group 11, which contains the noble metals Ag and Au. Traditional electronegativity scales, such as those of Pauling,¹ Allen,⁴⁵ or Mulliken,² all show the order $\text{Cu} < \text{Ag} < \text{Au}$. However, as is seen in Figure 3, the ordering is now $\text{Cu} < \text{Au} < \text{Ag}$. What to make of this apparent reversal in electronegativities? All the other electronegativity scales make gold the most electronegative element in groups 3–12. Not ours.

The reason for gold's resistance to oxidation, or "nobility", consistent with its high electronegativity, has been discussed by many.⁵² Indubitably, relativistic effects play a role in increasing gold's electronegativity,⁵³ and electronegativity has been invoked to explain gold's ability to take up electrons and form ionic salts with other metals.⁵⁴ But are electronegativity–reactivity arguments reasonable for gold, or a false friend? Indeed, whereas gold can react with a large variety of elements,^{55,56} gold oxides are not stable under ambient conditions.^{57,58} In the face of a very large difference in electronegativity between gold and oxygen (7.6 eV e^{-1} in this work, or 10.0 eV e^{-1} with Allen electronegativity), the nonexistence of stable gold oxides appears on the face of it as a conceptual failure of any common electronegativity scale, including our own. Looking at electronegativity differences alone, oxygen should most definitely oxidize gold!

The order obtained from our scale, $\text{Cu} < \text{Au} < \text{Ag}$, faces a further problem, for it leads one to expect that it is easier to oxidize gold than silver, which is certainly inconsistent with experience. To understand both discrepancies, we need to delve deeper into the effect of relativity, the "gold maximum".⁵⁹ Relativistic effects stabilize the 6s orbital of Au while destabilizing the 5d orbitals. The inertness of gold against oxidation stems in part from the inertness of the 6s electron,

which shares the same origin with the famous inert pair effect.^{60–62} Actually, the first ionization potential varies as 7.72, 7.58, and 9.22 eV from Cu to Ag and to Au, in good correspondence with the elements' resistance to oxidation. We will return to oxidation of group 11 atoms when we discuss conceptual failures of electronegativity in a future article.

■ ZINC, CADMIUM, AND MERCURY

The high electronegativities of Zn, Cd, and Hg that result from including their d^{10} subshells in the valence average should raise an eyebrow. Were we to change our definition (i.e., include for the elements only their occupied s orbitals in the configuration), the electronegativity of Zn, Cd, and Hg would drop significantly to 9.4, 9.0, and 10.4 eV e^{-1} , respectively.

Our preferred definition, based on an s^2d^{10} valence configuration, puts group 12 in a similar position to groups 2 and 18 and establishes that the atoms in the last groups of the s , p , and d blocks are the ones that hold their electrons the strongest. This observation is, in fact, mostly in agreement with the Mulliken definition of electronegativity (the average of the electron affinity and first ionization potential), in which Zn and Cd come out as the second and most electronegative transition metal atoms in their respective rows⁴⁵ and where the group 12 atoms are more electronegative than their counterparts in group 13 (Ga, In, Tl).

Cadmium emerges with our definition as the most electronegative of the d -block elements, ahead of zinc, mercury, and nickel (in that order). We can come to terms with this number in the following way; we think if electronegativity is seen as an indicator of resistance to oxidation, similar to how we discuss the noble gases, then a high electronegativity of group 12 atoms explains why Cd, with its high electronegativity of 16.1 eV e^{-1} , seemingly can reach an oxidation state of only +II, whereas, for example, iodine, with a lower electronegativity of 13.4 eV e^{-1} , can reach a formal oxidation state of +VII, in, for example, IF_7 . The electronegativities of Zn and Cd are similar, but slightly lower than that of Kr, 15.9, 16.1, and 17.4 eV e^{-1} , respectively. These values go well in hand with the fact that all of these atoms have a largest observed oxidation state of +II. Another example is Hg, which has a similar electronegativity to Xe, 14.1 and 14.9 eV e^{-1} , respectively. Both of these atoms can be oxidized to a +IV oxidation state, for example, in HgF_4 and XeF_4 . The existence of reduced group 12 elements, where these transition metal atoms occupy their p -levels, is also in agreement with their high electronegativities. Some examples here are dimeric Zintl anions in compounds of the type Ca_3Hg_2 and Ca_3M_3 ($M = Zn, Cd, \text{ and } Hg$).^{63,64}

Hg is a rather unique element: along with only Zn, Cd, Mn, Hf, Mg, Be, and the noble gas elements, it does not have a positive electron affinity. In the condensed state, Hg is also the only element of the transition metals that exists as a liquid state under ambient conditions, a consequence of strong relativistic effects and the resultant weak interatomic interactions. True, a 50 °C rise in the Earth's surface temperature would give us several other liquid elements, some with little role of relativity. The relatively high electronegativity of Hg can, similar to gold, in part be explained by the $6s$ binding energy, which is significantly increased by relativistic effects (the $6s$ ionization potential is 10.4 eV).

■ GROUP 10

Group 10 is an interesting one in general, as it illustrates how different atomic ground-state configurations can be: they are d^8s^2 for Ni, d^{10} for Pd, and s^1d^9 for Pt. When one moves to the respective cations, the d orbitals sink, and the cations of these elements are all d^9 . The fourth most electronegative atom of the d -block is nickel, here with an electronegativity of 12.9 eV e^{-1} .

■ MANGANESE AND TECHNETIUM

Most scales of electronegativity seem to disagree on Mn and Tc, which merits special comment. For example, in Allen's scale, the electronegativities of Mn and Tc fall in between their neighboring atoms of the same row. The older Pauling scale instead shows distinct "dips" in electronegativity at Mn and Tc when moving across the d -block. In our scale, Mn and Tc represent local maxima in electronegativity compared to their neighbors in the periodic table. There is a real distinction between the Pauling and our scales for Mn: in the Pauling scale Mn has the lowest electronegativity among the first-row transition elements Ti–Zn, while in our scale it has the third highest electronegativity (after Ni and Zn). Higher electronegativities for these atoms can be understood as a consequence of half-filled d -shells, which maximize exchange interactions between d electrons. This stabilization is removed upon ionization to the s^2d^4 configuration, which is necessary to define the d -binding energy.

The electronegativities of Mn and Tc are high compared to their neighbors, but not that high compared to nonmetals. We think it is feasible to reconcile this with experimental observation, it depends on how one argues. For example, the most stable oxidation state for Cr is +III, whereas for Mn it is +II. Iron most commonly exists in either +II or +III, intermediate in this respect between Cr and Mn. This series of most common (but not maximum) oxidation states is in agreement with electronegativities for Cr, Mn, and Fe of 8.0, 12.3, and 10.1 eV e^{-1} , respectively. The corresponding comparison between Mo, Tc, and Ru in the next row is not straightforward due to smaller relative differences in electronegativity between these atoms and a larger number of commonly occurring oxidation states in compounds of these atoms. The outliers in our scale compared to others will be studied in more detail in the future.

■ THE F-BLOCK

Before we proceed to discuss our results for the f -block, a comment on the computational methodology is in order. Except for Ac and Th, for which sufficient experimental data are available, the f -block electronegativities have been obtained from quantum-chemical calculations at the level of general multiconfigurational quasi-degenerate perturbation theory (GMC-QDPT), using the uncontracted ANO-RCC basis set. Our calculation results are summarized in Table 1 and compared with experimental data and CASPT2 results of Roos et al., which are denoted by different superscripts. Our calculated results are not denoted by superscripts.

Our non-spin–orbit coupling (non-SOC) calculated IPs compare favorably with those of Roos et al. Most of the deviations are smaller than 0.1 eV, reflecting the accuracy of our calculations. The largest deviation is 0.26 eV for the s IP of Am. The s ionization potential for Am calculated earlier at the CASPT2 level as 5.78 eV deviates more from the 5.97 eV

Table 1. Calculated Ionization Potentials of f-Block Elements^a

	configurations and $2s+1L_J$ states	s IP	d IP	f IP
Lanthanides				
Ce	$4f^1 5d^1 6s^2$; 1G_4 , $^2G_{9/2}$, $^2F_{5/2}$, $^2D_{3/2}$	5.73, 5.83 ^b	6.76, 6.75 ^b	11.13, 11.81 ^b
Pr	$4f^2 6s^2$; $^4I_{9/2}$, 5I_4 , 3G_4	5.37, 5.47; ^b 5.37, 5.35 ^c		7.51
Nd	$4f^3 6s^2$; 5I_4 , $^6I_{7/2}$, $^4I_{9/2}$	5.41, 5.53; ^b 5.41, 5.46 ^c		8.04
Pm	$4f^5 6s^2$; $^6H_{5/2}$, 7H_2 , 5I_4	5.44, 5.58; ^b 5.44, 5.49 ^c		8.21
Sm	$4f^6 6s^2$; 7F_0 , $^8F_{1/2}$, $^6H_{5/2}$	5.50, 5.64; ^b 5.49, 5.54 ^c		9.25
Eu	$4f^7 6s^2$; $^8S_{7/2}$, 9S_4 , 7F_0	5.53, 5.67; ^b 5.53, 5.68 ^c		10.49
Gd	$4f^7 5d^1 6s^2$; 9D_2 , $^{10}D_{5/2}$, $^8S_{7/2}$, $^8H_{3/2}$	6.06, 6.15; ^b 6.07, 5.92 ^c	6.82, 6.58 ^b	17.03
Tb	$4f^9 6s^2$; $^6H_{15/2}$, 7H_8 , 7F_6	5.86, 5.86; ^b 5.86, 5.86 ^c		8.11, 6.60 ^b
Dy	$4f^{10} 6s^2$; 5I_8 , $^6I_{17/2}$, $^6H_{15/2}$	5.94, 5.94; ^b 5.94, 5.93 ^c		8.84, 7.47 ^b
Ho	$4f^{11} 6s^2$; $^4I_{15/2}$, 5I_8 , 5I_8	6.02, 6.02; ^b 6.02, 6.01 ^c		8.73
Er	$4f^{12} 6s^2$; 3H_6 , $^4H_{13/2}$, $^4I_{15/2}$	6.09, 6.11; ^b 6.10, 6.08 ^c		7.85, 6.96 ^b
Tm	$4f^{13} 6s^2$; $^2F_{7/2}$, 3F_4 , 3H_6	6.17, 6.18; ^b 6.17, 6.17 ^c		9.44, 7.72 ^b
Yb	$4f^{14} 6s^2$; 1S_0 , $^2S_{1/2}$, $^2F_{7/2}$	6.25, 6.25; ^b 6.25, 6.21 ^c		10.75, 8.91 ^b
Actinides				
Pa	$5f^2 6d^1 7s^2$; $^4K_{11/2}$, 5K_5 , 3H_4 , 1G_4	6.02	6.13, 5.89; ^b 5.91, 5.96 ^c	6.72
U	$5f^3 6d^1 7s^2$; 5L_6 , $^6L_{11/2}$, $^4I_{9/2}$, $^4K_{11/2}$	6.12	6.33, 6.19; ^b 6.14, 6.16 ^c	8.78
Np	$5f^4 6d^1 7s^2$; $^6L_{11/2}$, 7L_5 , 5I_4 , 5L_6	6.17, 6.27; ^b 6.19, 6.17; ^c 6.17, 6.11 ^d	6.38	9.60
Pu	$5f^6 7s^2$; 7F_0 , $^8F_{1/2}$, $^6H_{5/2}$	5.96, 6.03; ^b 5.94, 5.80 ^c		7.69
Am	$5f^7 7s^2$; $^8S_{7/2}$, 9S_4 , 7F_0	6.04, 5.97; ^b 6.04, 5.78 ^c		8.96
Cm	$5f^7 6d^1 7s^2$; 9D_2 , $^{10}D_{5/2}$, $^8S_{3/2}$, $^8H_{3/2}$	6.49	6.32, 5.99; ^b 5.95, 5.83 ^c	12.79

^aGiven in the second column are the atomic ground-state configuration, followed by the $2s+1L_J$ level symbols of the atomic ground state and those of the lowest cationic states corresponding to the ionizations in the third to fifth columns in sequence. Our results are compared with available experimental data and the theoretical results reported in the literature.^{66,67} Different sets in the comparison are separated by a semicolon. Most of the s IPs reported in the literature do not contain spin-orbit coupling (SOC) corrections. Accordingly, our results compared with these values also do not contain SOC corrections. ^bExperimental ionization potentials from the NIST tables. ^cCASPT2 results without SOC of Roos et al. ^dCASPT2 results with SOC of Roos et al.

experimental result than our calculation of 6.04 eV. Please note that for this IP the inclusion of *LS*-coupled spin-orbit interaction does not change the outcome, because both the atomic ground state and the lowest s-ionized state are spatially nondegenerate and have no first-order SOC. Note also that

even for other atoms whose atomic ground states and lowest s-ionized states are spatially and spin-degenerate and both the atoms and the cations exhibit first-order SOC the inclusion of SOC in calculations does not change the results significantly, at most 0.02 eV (6.17 vs 6.19 eV for Np; 5.96 vs 5.94 eV for Pu). This is because the *ns* shell itself, which loses an electron in the s-ionization, does not experience SOC. On the other hand, the $(n-2)f$ and $(n-1)d$ shells experience SOC, but only the parts of their radial functions closest to the nucleus matter in spin-orbit coupling.⁶⁵ These innermost parts of the f and d orbitals are not much affected by the change of the s screening in the ionization. Our SOC-calculated s IPs agree satisfactorily with available experimental values, with the largest deviations of 0.14 eV. According to Roos et al., these errors are not untypical for multireference perturbation theory methods using their ANO-RCC basis sets.

Our calculated d and f IPs compare less favorably with experimental values. For the d IPs, the maximum deviation is 0.33 eV for Cm. For the f IPs, deviations of >1 eV are common. We attribute these larger errors to the *LS*-coupling treatment of the spin-orbit interaction. Unlike the s IPs, electrons in the d and f shells experience substantial SOC owing to their nonzero orbital angular momenta. For these heavy elements, their *J*-splittings deviate significantly from the Landé interval rule, and it is more appropriate to treat their strong SOC at the level of *jj* coupling. However, *jj* coupling calculations require two-component or four-component relativistic quantum chemistry programs. Such a program, with the occupation restricted multiple active space (ORMAS), is unavailable to us. We have therefore used our *LS*-coupling-based IPs to estimate the electronegativities. We emphasize the need for the ORMAS active space because of the convergence problem of using a complete active space (CAS): the specific $(n-2)f(n-1)d^j ns^k$ configuration is not preserved in self-consistent iterations (see the [Methodology](#) section).

Because of the limitations in accuracy of our SOC-GMC-QDPT IP calculations for treating f-ionization, we have to emphasize the qualitative nature of the electronegativities of the lanthanide and actinide elements shown in [Figure 3](#). Especially, when the f IPs are multiplied by the large number of f electrons in using [eq 2](#) to calculate the averaged binding energy, inherent errors are amplified.

Overall, and as expected, the electronegativities of the f-block atoms are mostly smaller than or similar to those of the d-block. The s^2d^1 atoms La and Ac have similar $\bar{\chi}$ values to those of Ca and Sr, respectively. As expected, half-filled and filled shells are stabilized, and the f^7 atoms Gd and Cm attain the highest electronegativities of the considered f-block atoms, 13.8 and 10.9 eV e⁻¹, respectively, which is similar in magnitude to the d^5 atoms Mn and Tc. Similarly, Yb, which has one filled f-shell, is predicted to have a similar electronegativity to that of Cu (10.2 eV e⁻¹).

Albeit not exact, we expect these electronegativities to be useful tools for predicting polarity and reactivity trends. For example, the recent experimental determination of the polarity of thorium–aluminum bonds⁶⁸ is in agreement with an electronegativity of 6.4 eV e⁻¹ for thorium and 9.1 eV e⁻¹ for aluminum.

■ WHEN ELECTRONEGATIVITY ARGUMENTS FAIL

Electronegativity is, as many chemists can attest, a fickle friend when it comes to predicting reactivity and charge transfer between atoms. While often it is a valuable guide, this central

chemical concept can also fail. Examples of such “conceptual failures” are dipole moments in diatomics that are opposite what can be expected from electronegativity arguments (CO, CF, BF, etc.), the nonexistence of thermodynamically stable compounds despite large electronegativity differences (such as gold oxides under ambient conditions), and trends in bond energies or reaction rates opposite what can be expected from classical arguments predicting polar bonds to be stronger. These seeming failures are or can be understood; we plan to address conceptual failures of electronegativity in a subsequent article.

For now, we end by highlighting that one appeal of the framework within which we define electronegativity here is the energy partitioning, written out as eq 1, where $\Delta\bar{\chi}$ is but one of several terms describing energetic preferences of reactions. Equation 1 only holds for all-electron averages, whereas the data presented herein (the new Table of Electronegativities) refer to valence averages. When electronegativity arguments fail in predicting a certain trend in energy, it can be concluded that either of two competing factors can be at play. Either the valence approximation fails and core-level shifts play a significant role in deciding the total energy change of a considered transformation, or, alternatively, changes in multi-electron interactions, summed in the ΔE_{ee} term of eq 1, which include electron correlation, govern the transformation.

As we shall show in future work, some apparent failures of the electronegativity concepts may not be failures at all, but an opportunity for chemists to gain additional insight into electronic structure–function relationships.

■ CONCLUSIONS

Electronegativity, $\bar{\chi}$, is here defined as the average binding energy of valence electrons in the ground state ($T \rightarrow 0$ K). This work represents a modification and expansion of the Allen scale of electronegativity, including all elements 1–96. Our definition is not limited to atoms and is, as we showed in previous work,²⁰ applicable to larger systems, such as molecules and condensed phase materials with extended electronic structures. The bulk of the presented data is experimental and taken from the NIST Atomic Spectra Database. Missing ionization potentials needed for the calculation of the ground-state electronegativities of several radioactive elements and most of the actinides and lanthanides have been obtained using quantum mechanical calculations.

The ground-state definition allows for the inclusion of essentially all the elements of chemical interest in a table of electronegativities. The values that emerge are in general slightly smaller than the configuration averages (which created difficulties for Allen). The correlation of our scale with Allen’s original one, and with other scales, is excellent. Choices have to be made with respect to valence levels; for the most part they are obvious, with obvious difficulties for group 12.

By and large the electronegativity of the atoms presented here agrees with conventional wisdom. For example, fluorine remains the most electronegative reactive element, but its numerical value is now in better agreement with experimental observations of noble gas fluorides. Some notable differences is that cadmium is now the most electronegative atom in the d-block, followed by Zn, Hg, Ni, Mn, Ag, Co, Tc, and Au, in that order. The heightened electronegativity of several d-block atoms relative to heavier p-block atoms in groups 13–15 suggests the possibility of alloys showing d-atom reduction and

p-atom oxidation. Indeed, a few such compounds have been observed, for example CoSb_3 .⁵¹

Electronegativity is a central chemical concept and a time-tested tool for guiding the design of new materials. We think that this revision and expansion of the electronegativity concept, which includes a framework for understanding its occasional failures, can lead the way to more reliable rationalization of cause and effect in chemical and physical transformations and a better understanding of electronic structure–function relationships.

■ METHODOLOGY

For the majority of elements we have compiled electronegativities from the most recent experimental data available through the NIST Atomic Spectra Database (physics.nist.gov). Exceptions include atoms Tc, Os, Po–Rn, La–Yb, and Ac, Pa–Cm, for which we to a varying degree have used quantum chemical calculations to estimate one or several valence ionization energies. A spin-orbit module⁶⁹ based on the GMC-QDPT method^{70–72} with an ORMAS⁷³ has been used to calculate energies of the relevant L – S terms and J levels of atoms and cations. These calculations were done using GAMESS-US.^{74,75} The active spaces contain ns and np orbitals for p-block elements, ns and $(n-1)d$ orbitals for d-block elements, and ns , $(n-1)d$, and $(n-2)f$ orbitals for f-block elements. The occupation schemes are identical to the targeted configurations; that is, minimum active spaces are used.

As shown by the comparison with results from CASPT2 in Table 1, the use of the minimum restricted active spaces does not give inferior results to those using complete active spaces. The use of the minimum ORMAS guarantees the MCSCF step, which prepares reference states for the subsequent PT treatment, to converge to the targeted states. We tried using CAS, but it quite often converges to states with lower energy, instead of the targeted L – S terms. Spin–orbit interaction was treated at the LS coupling level, except for Po–Rn. For the three p-block elements, the intermediate coupling scheme is employed, with all L – S terms arising from the respective atomic and cationic configurations included in the spin–orbit coupling calculations. All calculations were carried out using the uncontracted ANO-RCC basis sets.^{31,66,76} The third-order and the first-order Douglas–Kroll–Hess Hamiltonians^{77,78} were used to treat the scalar and spin–orbit relativistic effects, respectively.

■ ASSOCIATED CONTENT

Supporting Information

The Supporting Information is available free of charge on the ACS Publications website at DOI: 10.1021/jacs.8b10246.

Example calculation of $\bar{\chi}$ for Gd; valence binding energies (NIST or GMC-QDPT) used to calculate $\bar{\chi}$ for atoms 1–96; a list of $\bar{\chi}$ for atoms 1–96; comparison between $\bar{\chi}$ and Mulliken electronegativity (PDF)

■ AUTHOR INFORMATION

Corresponding Author

*martin.rahm@chalmers.se

ORCID

Martin Rahm: 0000-0001-7645-5923

Tao Zeng: 0000-0002-1553-7850

Road Hoffmann: 0000-0001-5369-6046

Notes

The authors declare no competing financial interest.

■ ACKNOWLEDGMENTS

M.R. acknowledges funding from the Swedish Research Council (2016-04127), Chalmers University of Technology, and computational resources provided by the Swedish

National Infrastructure for Computing (SNIC) at C3SE. T.Z. acknowledges funding from Carleton University (Start-up, 186853) and the Natural Sciences and Engineering Research Council (NSERC) of Canada (RGPIN-2016-06276) and computational resources provided by Compute Canada. Wojciech Grochala is thanked for comments and discussion.

REFERENCES

- (1) Pauling, L. Nature of the chemical bond. IV. The energy of single bonds and the relative electronegativity of atoms. *J. Am. Chem. Soc.* **1932**, *54*, 3570–3582.
- (2) Mulliken, R. S. New electroaffinity scale; together with data on valence states and on valence ionization potentials and electron affinities. *J. Chem. Phys.* **1934**, *2*, 782–793.
- (3) Gordy, W. A new method of determining electronegativity from other atomic properties. *Phys. Rev.* **1946**, *69*, 604–607.
- (4) Walsh, A. D. Factors affecting bond strengths. *Proc. R. Soc. London, Ser. A* **1951**, *207*, 13–30.
- (5) Sanderson, R. T. An interpretation of bond lengths and a classification of bonds. *Science* **1951**, *114*, 670–672.
- (6) Allred, A. L.; Rochow, E. G. A scale of electronegativity based on electrostatic force. *J. Inorg. Nucl. Chem.* **1958**, *5*, 264–268.
- (7) Iczkowski, R. P.; Margrave, J. L. Electronegativity. *J. Am. Chem. Soc.* **1961**, *83*, 3547–3551.
- (8) Sanderson, R. T. Electronegativity and bond energy. *J. Am. Chem. Soc.* **1983**, *105*, 2259–2261.
- (9) Pearson, R. G. Absolute electronegativity and absolute hardness of Lewis acids and bases. *J. Am. Chem. Soc.* **1985**, *107*, 6801–6806.
- (10) Allen, L. C. Electronegativity is the average one-electron energy of the valence-shell electrons in ground-state free atoms. *J. Am. Chem. Soc.* **1989**, *111*, 9003–9014.
- (11) Reed, J. L. Electronegativity: an atom in a molecule. *J. Phys. Chem.* **1991**, *95*, 6866–6870.
- (12) Ghosh, D. C. A new scale of electronegativity based on absolute radii of atoms. *J. Theor. Comput. Chem.* **2005**, *4*, 21–33.
- (13) Putz, M. V. Systematic formulations for electronegativity and hardness and their atomic scales within density functional softness theory. *Int. J. Quantum Chem.* **2006**, *106*, 361–389.
- (14) Politzer, P.; Peralta-Inga, S.; Zenaida; Bulat, F. A.; Murray, J. S. Average Local Ionization Energies as a Route to Intrinsic Atomic Electronegativities. *J. Chem. Theory Comput.* **2011**, *7*, 377–384.
- (15) Ferro-Costas, D.; Perez-Juste, I.; Mosquera, R. A. Electronegativity estimator built on QTAIM-based domains of the bond electron density. *J. Comput. Chem.* **2014**, *35*, 978–985.
- (16) Boyd, R. J.; Edgecombe, K. E. Atomic and group electronegativities from the electron-density distributions of molecules. *J. Am. Chem. Soc.* **1988**, *110*, 4182–4186.
- (17) Boyd, R. J.; Boyd, S. L. Group electronegativities from the bond critical point model. *J. Am. Chem. Soc.* **1992**, *114*, 1652–1655.
- (18) Jensen, W. B. Electronegativity from Avogadro to Pauling. Part I: origins of the electronegativity concept. *J. Chem. Educ.* **1996**, *73*, 11–20.
- (19) Jensen, W. B. Electronegativity from Avogadro to Pauling: II. Late nineteenth- and early twentieth-century developments. *J. Chem. Educ.* **2003**, *80*, 279–287.
- (20) Politzer, P.; Murray, J. S. Electronegativity—a perspective. *J. Mol. Model.* **2018**, *24*, 214.
- (21) Rahm, M.; Hoffmann, R. Toward an Experimental Quantum Chemistry: Exploring a New Energy Partitioning. *J. Am. Chem. Soc.* **2015**, *137*, 10282–10291.
- (22) Rahm, M.; Hoffmann, R. Distinguishing Bonds. *J. Am. Chem. Soc.* **2016**, *138*, 3731–3744.
- (23) Allen, L. C. Extension and completion of the periodic table. *J. Am. Chem. Soc.* **1992**, *114*, 1510–1511.
- (24) Allen, L. C. Chemistry and electronegativity. *Int. J. Quantum Chem.* **1994**, *49*, 253–277.
- (25) Mann, J. B.; Meek, T. L.; Allen, L. C. Configuration Energies of the Main Group Elements. *J. Am. Chem. Soc.* **2000**, *122*, 2780–2783.
- (26) Allen, L. C.; Knight, E. T. Electronegativity: why has it been so difficult to define? *J. Mol. Struct.: THEOCHEM* **1992**, *93*, 313–330.
- (27) Cotton, F. A.; Wilkinson, G.; Murillo, C. A.; Bochman, M. *Advanced Inorganic Chemistry*, 6th ed.; Wiley: New York, 1999.
- (28) Riedel, S.; Kaupp, M. The highest oxidation states of the transition metal elements. *Coord. Chem. Rev.* **2009**, *253*, 606–624.
- (29) Schlöder, T.; Kaupp, M.; Riedel, S. Can Zinc Really Exist in Its Oxidation State + III? *J. Am. Chem. Soc.* **2012**, *134*, 11977–11979.
- (30) Wang, X.; Andrews, L.; Riedel, S.; Kaupp, M. Mercury is a transition metal: the first experimental evidence for HgF₄. *Angew. Chem., Int. Ed.* **2007**, *46*, 8371–8375.
- (31) Roos, B. O.; Lindh, R.; Malmqvist, P.-A.; Veryazov, V.; Widmark, P. New relativistic ANO basis sets for actinide atoms. *Chem. Phys. Lett.* **2005**, *409*, 295–299.
- (32) Condon, E. U.; Shortley, G. H. *The Theory of Atomic Spectra*; Cambridge University Press: Cambridge, 1999.
- (33) Sessler, C. D.; Rahm, M.; Becker, S.; Goldberg, J. M.; Wang, F.; Lippard, S. J. CF₂H, a Hydrogen Bond Donor. *J. Am. Chem. Soc.* **2017**, *139*, 9325–9332.
- (34) Cárdenas, C.; Heidar-Zadeh, F.; Ayers, P. W. Benchmark values of chemical potential and chemical hardness for atoms and atomic ions (including unstable anions) from the energies of isoelectronic series. *Phys. Chem. Chem. Phys.* **2016**, *18*, 25721–25734.
- (35) Zaleski-Ejgierd, P.; Lata, P. M. Krypton oxides under pressure. *Sci. Rep.* **2016**, *6*, 18938–18938.
- (36) Olah, G. A.; Prakash, G. K. S.; Molnár, Á.; Sommer, J. *Superacid Chemistry*; John Wiley & Sons, Inc: Hoboken, NJ, 2009.
- (37) Christe, K. O. Chlorine trifluoride dioxide, ClF₃O₂. *Inorg. Nucl. Chem. Lett.* **1972**, *8*, 457–459.
- (38) Christe, K. O.; Curtis, E. C.; Dixon, D. A.; Mercier, H. P.; Sanders, J. C. P.; Schrobilgen, G. J. The pentafluoroxenate(IV) anion, XeF₅⁻: the first example of a pentagonal planar AX₅ species. *J. Am. Chem. Soc.* **1991**, *113*, 3351–3361.
- (39) O'Hagan, D. Understanding organofluorine chemistry. An introduction to the C-F bond. *Chem. Soc. Rev.* **2008**, *37*, 308–319.
- (40) Hunter, L. The C–F bond as a conformational tool in organic and biological chemistry. *Beilstein J. Org. Chem.* **2010**, *6*, 38.
- (41) Prakash, G. K. S.; Wang, F.; Zhang, Z.; Haiges, R.; Rahm, M.; Christe, K. O.; Mathew, T.; Olah, G. A. Long-Lived Trifluoromethanide Anion: A Key Intermediate in Nucleophilic Trifluoromethylations. *Angew. Chem., Int. Ed.* **2014**, *53*, 11575–11578.
- (42) Haiges, R.; Baxter, A. F.; Schaab, J.; Christe, K. O. Perfluoroalcohols: The Preparation and Crystal Structures of Heptafluorocyclobutanol and Hexafluorocyclobutane-1,1-diol. *Angew. Chem., Int. Ed.* **2018**, *57*, 8174–8177.
- (43) Dixon, D. A.; Wang, T.-H.; Grant, D. J.; Peterson, K. A.; Christe, K. O.; Schrobilgen, G. J. Heats of Formation of Krypton Fluorides and Stability Predictions for KrF₄ and KrF₆ from High Level Electronic Structure Calculations. *Inorg. Chem.* **2007**, *46*, 10016–10021.
- (44) Khriachtchev, L.; Pettersson, M.; Runeberg, N.; Lundell, J.; Rissanen, M. A stable argon compound. *Nature* **2000**, *406*, 874–877.
- (45) Mann, J. B.; Meek, T. L.; Knight, E. T.; Capitani, J. F.; Allen, L. C. Configuration Energies of the d-Block Elements. *J. Am. Chem. Soc.* **2000**, *122*, 5132–5137.
- (46) Lu, J.-B.; Jian, J.; Huang, W.; Lin, H.; Li, J.; Zhou, M. Experimental and theoretical identification of the Fe(VII) oxidation state in FeO₄⁻. *Phys. Chem. Chem. Phys.* **2016**, *18*, 31125–31131.
- (47) Kopelev, N. S.; Perfil'ev, Y. D.; Kiselev, Y. M. Moessbauer spectroscopy of iron oxo compounds in higher oxidation states. *J. Radioanal. Nucl. Chem.* **1992**, *157*, 401–414.
- (48) Perfiliev, Y. D.; Sharma, V. K. Higher oxidation states of iron in solid state: synthesis and their Mossbauer characterization. *ACS Symp. Ser.* **2008**, *985*, 112–123.
- (49) Gong, Y.; Zhou, M.; Kaupp, M.; Riedel, S. Formation and Characterization of the Iridium Tetroxide Molecule with Iridium in the Oxidation State + VIII. *Angew. Chem., Int. Ed.* **2009**, *48*, 7879–7883.

- (50) Wang, G.; Zhou, M.; Goettel, J. T.; Schrobilgen, G. J.; Su, J.; Li, J.; Schlöder, T.; Riedel, S. Identification of an iridium-containing compound with a formal oxidation state of IX. *Nature* **2014**, *514*, 475–475.
- (51) Stokkebro, S.; Mette; Bjerg, L.; Overgaard, J.; Krebs, L.; Finn; Hellerup, M.; Georg Kent; Sugimoto, K.; Takata, M.; Brummerstedt, I. Pushing X-ray Electron Densities to the Limit: Thermoelectric CoSb₃. *Angew. Chem., Int. Ed.* **2013**, *52*, 1503–1506.
- (52) Alcantara, O. M.; Stolbov, S. The perturbation energy: A missing key to understand the “nobleness” of bulk gold. *J. Chem. Phys.* **2015**, *142*, 194705.
- (53) Schwerdtfeger, P.; Dolg, M.; Schwarz, W. H. E.; Bowmaker, G. A.; Boyd, P. D. W. Relativistic effects in gold chemistry. I. Diatomic gold compounds. *J. Chem. Phys.* **1989**, *91*, 1762–1774.
- (54) Smetana, V.; Rhodehouse, M.; Meyer, G.; Mudring, A.-V. Gold Polar Intermetallics: Structural Versatility through Exclusive Bonding Motifs. *Acc. Chem. Res.* **2017**, *50*, 2633–2641.
- (55) Rahm, M.; Hoffmann, R.; Ashcroft, N. W. Ternary Gold Hydrides: Routes to Stable and Potentially Superconducting Compounds. *J. Am. Chem. Soc.* **2017**, *139*, 8740–8751.
- (56) Schmidbaur, H. The Auophilicity Phenomenon: A Decade of Experimental Findings, Theoretical Concepts and Emerging Applications. *Theoretical Concepts and Emerging Applications, Gold Bulletin* **2000**, *33*, 3–10.
- (57) Hermann, A.; Derzsi, M.; Grochala, W.; Hoffmann, R. AuO: Evolving from Dis- to Comproportionation and Back Again. *Inorg. Chem.* **2016**, *55*, 1278–1286.
- (58) Tsai, H.; Hu, E.; Perng, K.; Chen, M.; Wu, J.-C.; Chang, Y.-S. Instability of gold oxide Au₂O₃. *Surf. Sci.* **2003**, *537*, L447–L450.
- (59) Pyykkö, P. Theoretical chemistry of gold. *Angew. Chem., Int. Ed.* **2004**, *43*, 4412–4456.
- (60) Grimm, H. G.; Sommerfeld, A. Über den Zusammenhang des Abschlusses der Elektronengruppen im Atom mit den chemischen Valenzzahlen. *Eur. Phys. J. A* **1926**, *36*, 36–59.
- (61) Sidgwick, N. V. *The Electronic Theory of Valency*; Oxford: Clarendon, 1927.
- (62) Kaupp, M. Chemical bonding of main-group elements. *Chem. Bond* **2014**, *2*, 1–24.
- (63) Köhler, J.; Whangbo, M.-H. Late transition metal anions acting as p-metal elements. *Solid State Sci.* **2008**, *10*, 444–449.
- (64) Lee, C.; Whangbo, M.-H.; Köhler, J. Analysis of Electronic Structures and Chemical Bonding of Metal-rich Compounds. 2. Presence of Dimer (T-T)₄⁻ and Isolated T₂⁻ Anions in the Polar Intermetallic Cr₅B₃-Type Compounds AE₅T₃ (AE = Ca, Sr; T = Au, Ag, Hg, Cd, Zn). *Z. Anorg. Allg. Chem.* **2010**, *636*, 36–40.
- (65) Zeng, T.; Fedorov, D. G.; Klobukowski, M. Multireference study of spin-orbit coupling in the hydrides of the 6p-block elements using the model core potential method. *J. Chem. Phys.* **2010**, *132*, 1–15.
- (66) Roos, B. O.; Lindh, R.; Malmqvist, P.; Veryazov, V.; Widmark, P.; Borin, A. C. New Relativistic Atomic Natural Orbital Basis Sets for Lanthanide Atoms with Applications to the Ce Diatom and LuF₃. *J. Phys. Chem. A* **2008**, *112*, 11431–11435.
- (67) Roos, B. O.; Lindh, R.; Malmqvist, P.-A.; Veryazov, V.; Widmark, P. New relativistic ANO basis sets for actinide atoms. *Chem. Phys. Lett.* **2005**, *409*, 295–299.
- (68) Altman, A. B.; Brown, A. C.; Rao, G.; Lohrey, T. D.; Britt, R. D.; Maron, L.; Minasian, S. G.; Shuh, D. K.; Arnold, J. Chemical structure and bonding in a thorium(III)-aluminum heterobimetallic complex. *Chem. Sci.* **2018**, *9*, 4317–4324.
- (69) Zeng, T. A diabatisation protocol that includes spin-orbit coupling. *J. Chem. Phys.* **2017**, *146*, 144103.
- (70) Nakano, H.; Uchiyama, R.; Hirao, K. Quasi-degenerate perturbation theory with general multiconfiguration self-consistent field reference functions. *J. Comput. Chem.* **2002**, *23*, 1166–1175.
- (71) Miyajima, M.; Watanabe, Y.; Nakano, H. Relativistic quasidegenerate perturbation theory with four-component general multiconfiguration reference functions. *J. Chem. Phys.* **2006**, *124*, 044101.
- (72) Ebisuzaki, R.; Watanabe, Y.; Nakano, H. Efficient implementation of relativistic and non-relativistic quasidegenerate perturbation theory with general multiconfigurational reference functions. *Chem. Phys. Lett.* **2007**, *442*, 164–169.
- (73) Ivanic, J. Direct configuration interaction and multiconfigurational self-consistent-field method for multiple active spaces with variable occupations. I. Method. *J. Chem. Phys.* **2003**, *119*, 9364–9376.
- (74) Schmidt, M. W.; Baldrige, K. K.; Boatz, J. A.; Elbert, S. T.; Gordon, M. S.; Jensen, J. H.; Koseki, S.; Matsunaga, N.; Nguyen, K. A.; Su, S.; Windus, T. L.; Dupuis, M.; Montgomery, J. A. General Atomic and Molecular Electronic Structure System. *J. Comput. Chem.* **1993**, *14*, 1347–1363.
- (75) Gordon, M. S.; Advances, M. W. S. In *Electronic structure theory: GAMESS a decade later. Theory and Applications of Computational Chemistry: the first forty years*; Elsevier Science, 2005; pp 1167–1189.
- (76) Roos, B. O.; Lindh, R.; Malmqvist, P.-A.; Veryazov, V.; Widmark, P. New Relativistic ANO Basis Sets for Transition Metal Atoms. *J. Phys. Chem. A* **2005**, *109*, 6575–6579.
- (77) Hess, B. A. Relativistic electronic-structure calculations employing a two-component no-pair formalism with external-field projection operators. *Phys. Rev. A: At., Mol., Opt. Phys.* **1986**, *33*, 3742–3748.
- (78) Douglas, M.; Kroll, N. M. Quantum electrodynamicical corrections to the fine structure of helium. *Ann. Phys. (Amsterdam, Neth.)* **1974**, *82*, 89–155.